

Reaction $\pi^-p \rightarrow \pi^- \pi^+ n$ at 8 GeV/c

J. A. POIRIER, N. N. BISWAS, N. M. CASON, I. DERADO,* V. P. KENNEY,
W. D. SHEPHARD, AND E. H. SYNNT†

Department of Physics, University of Notre Dame, Notre Dame, Indiana‡

AND

H. YUTA,§ W. SELOVE, R. EHRlich,|| AND A. L. BAKER

*Department of Physics, University of Pennsylvania, Philadelphia, Pennsylvania***

(Received 22 June 1967)

Approximately 26 500 two-prong events were measured and analyzed by the Notre Dame and Pennsylvania groups, independently. From these analyses, 2421 events of the reaction $\pi^-p \rightarrow \pi^- \pi^+ n$ were obtained. The predictions of one-particle-exchange models with and without absorptive effects are compared with our data for the production and decay of the ρ^0 and the f^0 . We have also observed the recently discovered g^0 meson. The cross sections for ρ^0 , f^0 , and g^0 production are also given.

I. INTRODUCTION

DURING the past few years, studies of single-pion production in pion-nucleon interactions have provided better understanding of the production mechanism. In particular, the refined one-pion-exchange theory with absorptive effects (OPEA) has been successful in predicting both production and decay processes in various interactions. Studies of the production and decay of existing resonances in higher-energy interactions would furnish further tests of these theories.

In this paper we present an analysis of 2421 events of the type

$$\pi^-p \rightarrow \pi^- \pi^+ n \quad (1)$$

produced in 8-GeV/c π^-p interactions. A major part of the discussion concerns production and decay of the ρ^0 and the f^0 resonances; we remark on the recently discovered g^0 resonance.

Data presented here were combined from two separate experiments in the Brookhaven 80-in. hydrogen bubble chamber by Notre Dame and Pennsylvania groups. In the University of Notre Dame experiment, at an incident beam momentum of 8.05 GeV/c, about 20 500 two-prong events have been measured and 1321 events have been identified as reaction (1) on the basis of HGEOM-GRIND fits. In the University of Pennsylvania experiment at 7.9 GeV/c, about 6000 two-prong events were selected from a special scan¹ with criteria which exclude most types of two-prong events in which the positive outgoing track is a proton; 1100 events of reaction (1) have been identified on the basis of TRED-KICK fits. Selection criteria for reaction (1) in both experiments are as follows:

* Present address: Stanford Linear Accelerator Center, Stanford, California.

† Present address: Physics Department, King's College, Wilkes-Barre, Pennsylvania.

‡ Work supported in part by the National Science Foundation.

§ Present address: Physics Department, University of Rochester, Rochester, New York.

|| Present address: Physics Department, Rutgers, The State University, New Brunswick, New Jersey.

** Work supported in part by the U. S. Atomic Energy Commission.

¹H. Yuta, University of Pennsylvania, 1966 (unpublished); E. H. Synn, thesis, University of Notre Dame, 1966 (unpublished).

- (a) There is no allowed elastic fit,
- (b) the ionization of the positive particle is consistent with the fitted momentum,
- (c) the χ^2 probability for reaction (1) is greater than 1% (Notre Dame) or 5% (Pennsylvania), and
- (d) the square of the missing mass is in the interval from 0.30 to 1.50 GeV² (Notre Dame) or from 0.30 to 1.44 GeV² (Pennsylvania).

We estimate about 10% contamination from misclassified events of type $\pi^-p \rightarrow \pi^- \pi^+ n(\pi^0)$ and about 10% loss from events misclassified into the same type. Contamination due to high-momentum-proton events was estimated¹ to be about 1.5%.

In the Pennsylvania data, there is some bias¹ in a high $\pi\pi$ mass region [$M(\pi^+, \pi^-)$ greater than about 1500 MeV] because of the special scanning criteria. It appears that 100 to 200 events have been lost, nearly all of them having $M(\pi^+, \pi^-)$ greater than about 1500 MeV and also having a low π^+ laboratory momentum. Because of this effect, caution must be used in drawing detailed conclusions from the combined data above 1500 MeV. To make the data compatible for comparison purposes, we have analyzed the events in ways similar to those used for previous experiments at lower momenta.²

II. GENERAL FEATURES OF THE REACTION

Figure 1 shows the $\pi^- \pi^+$ invariant mass spectrum for reaction (1). Figure 1(a) is the Pennsylvania data, Fig. 1(b) is the Notre Dame data, and Fig. 1(c) is the combined data. The ρ^0 and the f^0 resonances are prominent: About 24% of the events correspond to ρ^0 production and 17% to f^0 production. The g^0 meson³ at 1650 MeV is observed as a peak standing more than 4

²Aachen-Birmingham-Bonn-Hamburg-London (I. C.)-München Collaboration, Nuovo Cimento **31**, 729 (1964); V. Hagopian, W. Selove, J. Alitti, J. P. Baton, and M. Neveu-René, Phys. Rev. **145**, 1128 (1966); V. Hagopian and Y. L. Pan, *ibid.* **152**, 1183 (1966).

³For a discussion of the g^0 meson and for references to the original report and subsequent reports on it, see G. Goldhaber, in *Proceedings of the Thirteenth Annual International Conference on High-Energy Physics, Berkeley, California, 1966* (University of California Press, Berkeley, California, 1967).

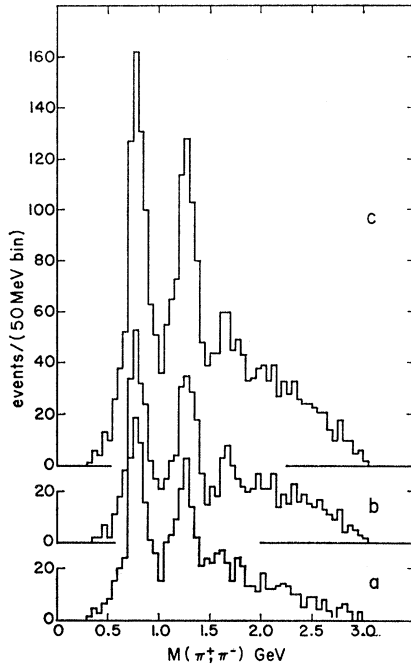


FIG. 1. $\pi^+\pi^-$ mass spectrum (a) for the Pennsylvania data, 1100 events; (b) for the Notre Dame data, 1321 events; and (c) for the combined data, 2421 events.

standard deviations above the nonresonant background (about 60 events above 150 background events from 1550 to 1750 MeV). In Fig. 2 are shown the combined $\pi^+\pi^-$ mass distributions for different ranges of Δ^2 .

In order to show possible isobar effects for the $\pi^+\pi^-$ mass distribution, Fig. 3 shows a Dalitz plot for the 2421 $\pi^-\pi^+n$ events. The ρ^0 and the f^0 appear as prominent horizontal bands at about 0.60 and 1.57 GeV^2 ; the g^0 band just under 3 GeV^2 is less clear. For $\pi^+\pi^-$ masses above the g^0 , events are concentrated at low π^+n mass. This concentration of events for higher $\pi\pi$ mass is

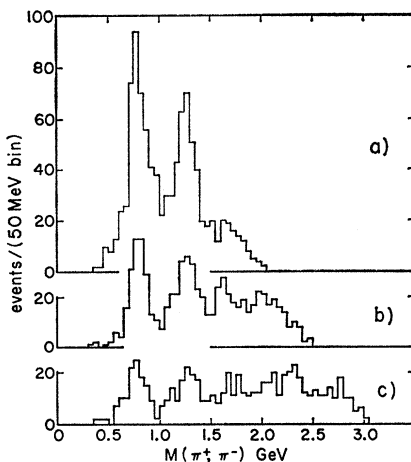


FIG. 2. Combined $\pi^+\pi^-$ mass distributions for (a) $0 < \Delta^2 < 5\mu^2$, 977 events, (b) $5 < \Delta^2 < 15\mu^2$, 736 events, and (c) $\Delta^2 > 15\mu^2$, 708 events. Here μ is the rest mass of the charged π meson, Δ^2 is the four-momentum transfer between initial and final nucleon, squared.

associated with the clustering of events at $\cos\theta$ near +1.0 (see Fig. 5 and the discussion below). From Fig. 3, we see no evidence of π^-n isobar production⁴; π^+n isobar effects are not prominent. The absence of π^-n isobar effects could be explained in an exchange model where the exchanged particle would have to be either doubly charged or a nucleon.⁵ Other evidence suggests that such exchanges are relatively weak.⁶

In order to show the general features of the momentum-transfer distribution, we show the Chew-Low plot of $M(\pi^+\pi^-)$ versus Δ/μ for reaction (1) in Fig. 4. Here Δ is the four-momentum transfer between initial and final nucleon, and μ is the charged π rest mass. This plot shows that (a) most events occur near the minimum allowed Δ , (b) there is a large middle range of Δ in which there are very few events, and (c) there

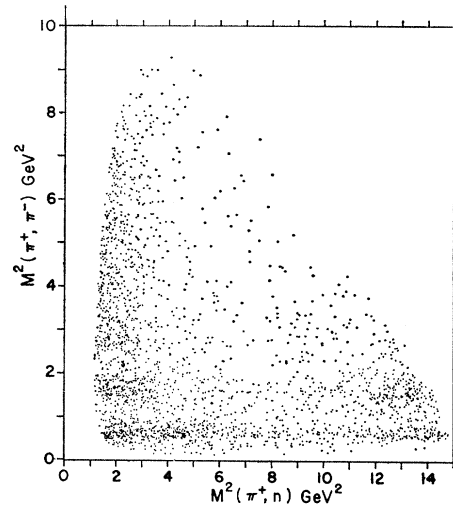


FIG. 3. Dalitz plot for all $\pi^+\pi^-n$ events.

are a few events at backward production angles (i.e., along the upper boundary of the allowed region), which may correspond to baryon exchange.

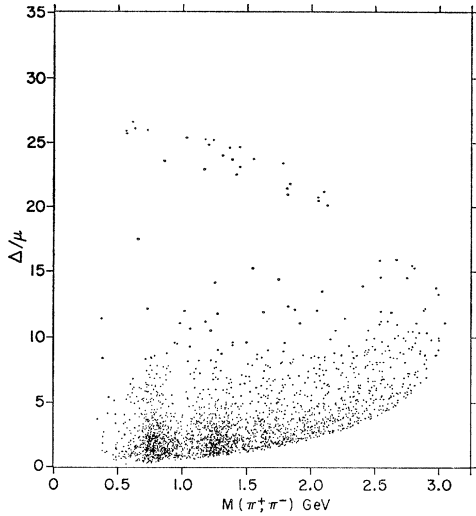
Figure 5 shows the $\cos\theta$ distribution as a function of the $\pi^+\pi^-$ invariant mass, where θ is the angle between the incident π^- and the final π^- in the dipion rest system. This plot shows that (a) there is a strong forward-backward asymmetry for the ρ^0 region which is similar to that observed at lower energies, (b) the distribution is rather symmetrical for the f^0 region, and (c) there is a strong tendency toward forward scattering for high $\pi\pi$ mass.

The total cross section for the reaction $\pi^- p \rightarrow \pi^+\pi^-n$ has been determined in two ways. At Notre Dame a

⁴ π^-n isobar effects would appear as a diagonal band in this plot. The position of this band shifts slightly for the two sets of data due to small differences in the incident beam momentum.

⁵ Y. Y. Lee, B. P. Roe, D. Sinclair, and J. C. Vander Velde, Phys. Rev. Letters **12**, 342 (1964).

⁶ Aachen-Berlin-Birmingham-Bonn-Hamburg-London (I. C.)-München Collaboration, Phys. Rev. **138**, B897 (1965); J. Orear, R. Rubenstein, D. B. Scarf, D. H. White, A. D. Krisch, W. R. Frisken, A. L. Read, and H. Ruderman, Phys. Rev. Letters **15**, 309 (1965).

FIG. 4. Chew-Low plot for $\pi^+\pi^-$.

value was obtained by considering (a) the pion path length corrected for beam contamination, flare loss, and geometry; (b) the density of the expanded hydrogen; and (c) the number of events in the fiducial volume corrected for scanning efficiency, event selection criteria, unmeasurable events, and systems losses. The total cross section for all 8-GeV/c π^-p interactions, computed in this manner, is 28.4 ± 1.7 mb, which agrees with the Brookhaven counter value⁷ of 27.5 ± 0.3 mb. At Pennsylvania a value was obtained by starting with the counter value for the total cross section and multiplying by the ratio of observed two-prong events to events of all topologies in order to obtain the cross section for all two-prong interactions. This quantity was then divided among the various two-prong channels according to the relative numbers of events identified in a sample of 2500 events. Corrections were applied for events with short proton tracks and steeply dipping tracks.

The total cross sections for the $\pi^-\pi^+n$ channel determined by the two procedures are given in Table I. They differ by about 2.5 standard deviations, which could be due to systematic uncertainties. The weighted average of the two cross-section values is shown in Table I, and is used to calculate the partial cross sections quoted in the following discussion. It should be noted that the error given is statistical only, and does not include any estimate of systematic errors.

The masses and widths for the ρ^0 , f^0 , and g^0 mesons, summarized in Table I, have been determined by maximum-likelihood fits to the data. We have used three-body phase space to approximate the background and constant-width Breit-Wigner curves (times phase space) to approximate the ρ^0 , f^0 , and g^0 . For the case of the ρ^0 and f^0 , only dipion masses below 1.7 GeV were

⁷ W. Galbraith, E. W. Jenkins, T. F. Kycia, B. A. Leontic, R. H. Phillips, A. L. Read, and R. Rubenstein, Phys. Rev. **138**, B913 (1965).

TABLE I. Parameters for the reaction $\pi^-p \rightarrow \pi^-\pi^+n$ at 8 GeV/c.^a

	σ (mb)	M_0 (GeV)	Γ (GeV)
All events, Notre Dame	0.89 ± 0.05		
All events, Pennsylvania	1.08 ± 0.08		
All events, weighted average	0.96 ± 0.05		
$\rho^0 \rightarrow \pi^+\pi^-$, combined	0.234 ± 0.021	0.777 ± 0.005	0.135 ± 0.010
$f^0 \rightarrow \pi^+\pi^-$, combined	0.165 ± 0.018	1.262 ± 0.007	0.163 ± 0.016
$g^0 \rightarrow \pi^+\pi^-$, combined	0.054 ± 0.013	1.680 ± 0.020	$0.226_{-0.046}^{+0.068}$

^a Errors are statistical only, and do not reflect the correlations among the variables used in the fit.

used in the combined fit; for the g^0 -meson, the mass interval 1.5 to 1.9 GeV was used. The central mass values and widths with their errors as determined from the fit are shown in Table I. We also tried Breit-Wigner curves with mass-dependent widths⁸ in the fitting procedure; the masses and widths were the same, within errors.

The production cross sections for the ρ^0 , f^0 , and g^0 were determined in the following way. To obtain the cross section for ρ^0 production, the area of the fitted Breit-Wigner curve for the ρ^0 is divided by the corrected total number of events for reaction (1); multiplying this by the total cross section of 0.960 mb yields 0.234 mb for the total production cross section for $\rho^0 \rightarrow \pi^+\pi^-$. The error on the ρ^0 cross section is obtained by taking the fitted error for the area of the constant-width Breit-Wigner curve folded with the error in the total cross section. The production cross sections for $f^0 \rightarrow \pi^+\pi^-$ and $g^0 \rightarrow \pi^+\pi^-$ were similarly obtained. For the case of the g^0 , however, because of the previously mentioned bias in the high dipion mass region, the cross section is probably underestimated by about 10%. The use of a mass-dependent-width Breit-Wigner curve yields higher cross sections for resonance production.

III. ρ^0 MASS REGION

A. Δ^2 Distribution of the Production Cross Section

Figure 6 shows the Δ^2 distribution of the ρ^0 production cross section. The ρ^2 mass interval was taken from 675 to 875 MeV. About 19% of the events in this mass region are non- ρ events. The absolute scale has been normalized to our estimate of the total cross section for ρ^0 production given in Table I.

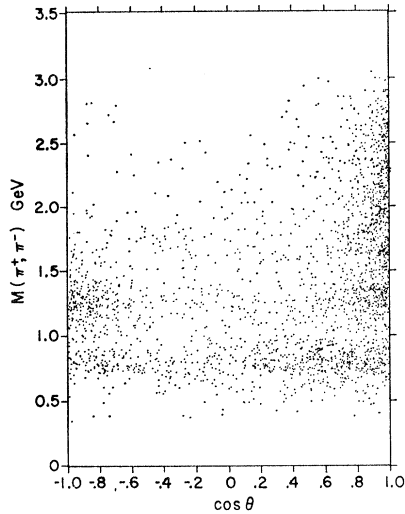
The theoretical curves in Fig. 6 are (a) one-pion exchange (OPE),⁹ (b) one-pion exchange with form factors (OPEF),¹⁰ and (c) one-pion exchange with absorption (OPEA).¹¹ It is seen that both (b) and (c) give good fits to the production distribution. It should be noted, however, that the OPEF model does not

⁸ J. D. Jackson, Nuovo Cimento **34**, 1644 (1964).

⁹ K. Gottfried and J. D. Jackson, Nuovo Cimento **34**, 735 (1964); J. D. Jackson, Rev. Mod. Phys. **37**, 484 (1965); J. D. Jackson, J. T. Donohue, K. Gottfried, R. Keyser, and B. E. Y. Svensson, Phys. Rev. **139**, B428 (1965).

¹⁰ F. Selleri, Phys. Letters **3**, 76 (1962).

¹¹ J. D. Jackson, Nuovo Cimento **34**, 1644 (1964); J. T. Donohue and J. D. Jackson (private communication).

FIG. 5. Scatter plot of $\cos\theta$ versus $M(\pi\pi)$.

predict the diagonal correlation between $\cos\theta$ and α discussed in the next section, which is predicted by OPEA.

B. Decay Angular Distributions

In Fig. 7 we show a scatter plot of the cosine of the dipion decay angle⁹ θ versus the Treiman–Yang angle¹² α , together with the projections on the axes. This figure shows the distinctive diagonal correlation in the decay variables and the related asymmetries in the projections which have also been observed at lower beam momenta. The asymmetry parameter in $\cos\theta$, $(F-B)/(F+B)$, is 0.30 ± 0.04 , where F and B are the numbers of events with $\cos\theta > 0$ and $\cos\theta < 0$, respectively. (For $\Delta^2 \leq 15 \mu^2$, the ratio is 0.33 ± 0.05 .) The asymmetries in

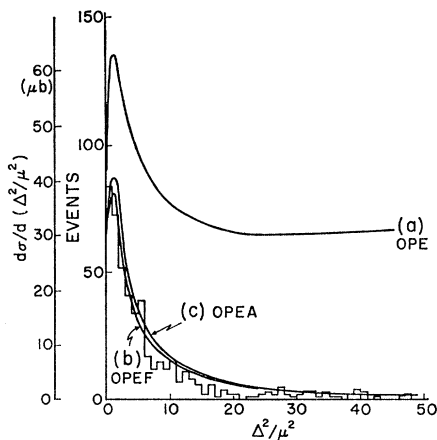


FIG. 6. Production cross section $d\sigma/d(\Delta^2/\mu^2)$ for the ρ^0 region. The solid curves are the predictions of (a) pure one-pion exchange, (b) one-pion exchange with form factor, and (c) one-pion exchange with absorption. A ρ^0 width of 135 MeV was used in these calculations.

¹² S. B. Treiman and C. N. Yang, Phys. Rev. Letters 8, 140 (1962).

the projections cannot be explained in terms of pure ρ^0 decay ($J^P=1^-$) even when OPEA is applied. The neutral ρ data may be contrasted with charged ρ decay, both at 8 GeV/c and at lower beam momenta, in which no asymmetries are observed.

It is interesting to note that diagonal correlations, and the value of $\text{Re}(\rho_{10})$, have approximately the same character at 8 GeV/c as at lower beam momenta.^{2,13} Recent theoretical studies of Reggeized exchange for the reaction $\pi^- p \rightarrow \rho^0 n$ indicate that the experimental values of the pure p -wave ρ density matrix elements and the t distribution of the ρ production cross section can be fitted for $\Delta^2 \lesssim 15 \mu^2$ by including π and A_2 exchange.¹⁴

If s - and p -wave $\pi\pi$ interactions are considered, the

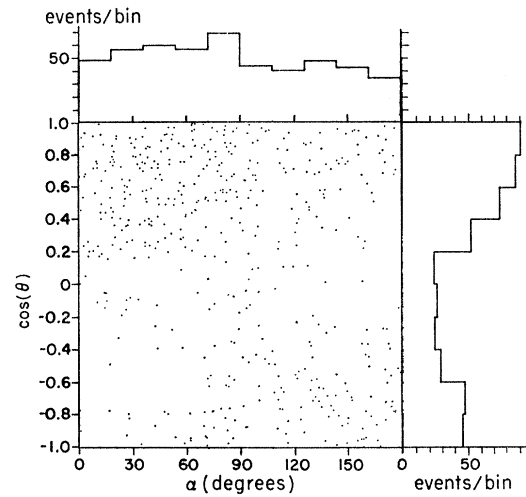


FIG. 7. Scatter plot of $\cos\theta$ versus α for the ρ^0 region with histogram projections on the $\cos\theta$ and α axes.

decay distribution may be described in terms of density matrix elements ρ_{mn} in the following form^{13,15}:

$$W(\theta, \alpha) = (3/4\pi) [\rho_{00} \cos^2\theta + \rho_{11} \sin^2\theta - \sqrt{2} \text{Re}(\rho_{10}) \times \sin 2\theta \cos\alpha - \rho_{1-1} \sin^2\theta \cos 2\alpha] + (\sqrt{3}/4\pi) \times [-2\sqrt{2} \text{Re}(\rho_{10}^{\text{int}}) \sin\theta \cos\alpha + 2 \text{Re}(\rho_{00}^{\text{int}}) \cos\theta] + (1/4\pi) [\rho_{00}^s]. \quad (2)$$

In this equation ρ_{00}^s corresponds to pure s -wave effects and ρ_{00}^{int} and ρ_{10}^{int} correspond to s - p interference effects. The ratio of intensities of s and p waves is given by

$$S/P = \rho_{00}^s / (\rho_{00} + 2\rho_{11}). \quad (3)$$

With the use of the normalization condition

$$\rho_{00} + 2\rho_{11} + \rho_{00}^s = 1, \quad (4)$$

¹³ I. Derado, V. P. Kenney, J. A. Poirier, and W. D. Shephard, Phys. Rev. Letters 14, 872 (1965).

¹⁴ R. Torgerson (private communication).

¹⁵ L. J. Gutay, P. B. Johnson, F. J. Loeffler, R. L. McAlwain, D. H. Miller, R. B. Willmann, and P. L. Csonka, Phys. Rev. Letters 18, 142 (1967).

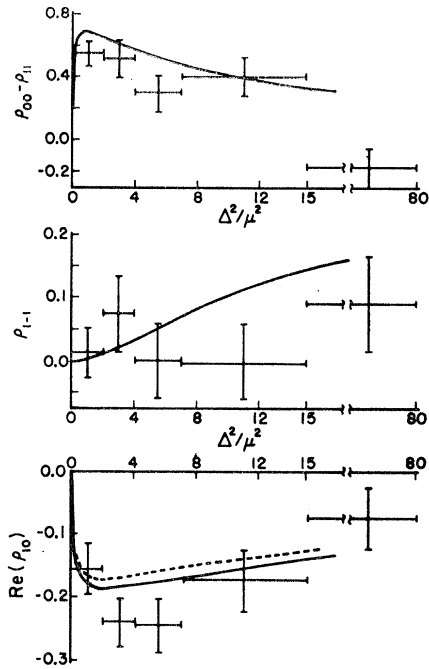


FIG. 8. Density matrix elements ($\rho_{00}-\rho_{11}$), $\text{Re}(\rho_{10})$, and $\rho_{1,-1}$. The solid curves are predictions of the OPEA model based on pure p -wave interaction; the dashed curve is based on the OPEA model with the addition of an s -wave resonance in the ρ^0 region. The solid and dashed curves overlap in the top two figures.

the explicit dependence of function (2) on ρ_{00}^* may be eliminated. The relevant quantities which may be determined experimentally are $(\rho_{00}-\rho_{11})$, $\text{Re}(\rho_{10})$, $\rho_{1,-1}$, $\text{Re}(\rho_{10}^{\text{int}})$, and $\text{Re}(\rho_{00}^{\text{int}})$. We have obtained values for these elements from the experimental decay distributions by the least-squares method. Figures 8 and 9 show the momentum-transfer dependence of the matrix elements. The solid curves in Fig. 8 are theoretical predictions calculated from the OPEA model¹¹ neglecting any s -wave contribution. In comparing these curves with the experimental data, two factors must be kept in mind: (1) We have not made any corrections for non- ρ background, estimated to be 19% of the total events, and (2) allowance must be made for the presence of a possible s -wave contribution. To take account of an s -wave contribution, the experimental values in Fig. 8 should be compared with $P/(S+P)$ times the theoretical "pure p -wave" ($S=0$) curves. The experimental points are in reasonable agreement with the "pure p -wave" curves; however, they are also consistent with an s -wave contribution of a few percent. The nonzero values for $\text{Re}(\rho_{00}^{\text{int}})$ (which is a very sensitive test for the presence of small amounts of s wave) shown in Fig. 9 are a strong indication of the presence of s -wave effects. Theoretically, $\text{Re}(\rho_{00}^{\text{int}})$ is simply related to the forward-backward asymmetry in $\cos\theta$: $(F-B)/(F+B) = \sqrt{3} \text{Re}(\rho_{00}^{\text{int}})$.

The dashed curves in Figs. 8 and 9 represent a calculation by Jabbur¹⁶ based on the OPEA model where

¹⁶ R. J. Jabbur (private communication).

TABLE II. Density matrix elements obtained for 8-GeV/ c fits to the ρ^0 decay angle distributions (all Δ^2).

Matrix element	Experiment	OPEA prediction
$\rho_{00}-\rho_{11}$	0.377 ± 0.050	0.557
$\text{Re}(\rho_{10})$	-0.178 ± 0.020	-0.174
$\rho_{1,-1}$	0.033 ± 0.025	0.047
$\text{Re}(\rho_{10}^{\text{int}})$	-0.048 ± 0.014	
$\text{Re}(\rho_{00}^{\text{int}})$	0.169 ± 0.024	

he has assumed the presence of an s -wave resonance in the ρ region. These particular curves were calculated assuming an s -wave resonance with the same mass and width as the ρ . The calculation is described in Ref. 17 by Griffiths and Jabbur. Although the experimental evidence¹⁸ suggests that these parameters for the resonance may not be reasonable, the curves indicate qualitatively the effects which may arise from an s -wave contribution. Further discussion is contained in Sec. IIIC.

In Table II are listed values for the density matrix elements averaged over all momentum transfers. For comparison, values calculated for the OPEA (p -wave only) model are presented. The ρ^0 matrix elements, when compared with the OPEA predictions, give $\chi^2 = 13$ for 3 degrees of freedom; this contrasts with $\chi^2 = 39$ obtained for the ρ^- matrix elements at the same energy.¹⁹

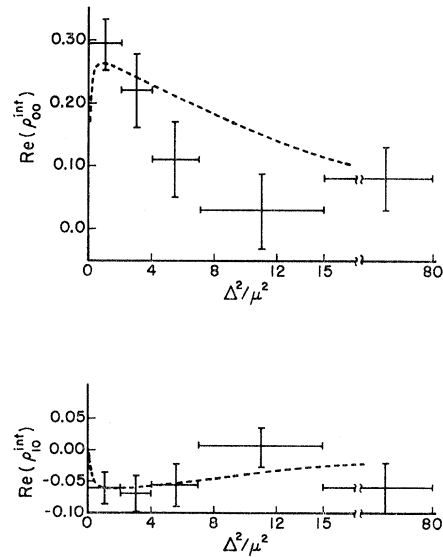


FIG. 9. Interference density matrix elements $\text{Re}(\rho_{00}^{\text{int}})$ and $\text{Re}(\rho_{10}^{\text{int}})$ for the ρ^0 region. The dashed curves are predictions of the OPEA model with the addition of an s -wave resonance in the ρ^0 region.

¹⁷ David Griffiths and R. J. Jabbur, *Phys. Rev.* **157**, 1371 (1967).

¹⁸ M. Feldman, W. Frati, J. Halpern, A. Kanofsky, M. Nussbaum, S. Richert, P. Yamin, A. Choudry, S. Devons, and J. Grunhaus, *Phys. Rev. Letters* **14**, 869 (1965); V. Hagopian, W. Selove, J. Alitti, J. P. Baton, M. Neveu-René, R. Gessaroli, and A. Romano, *ibid.* **14**, 1077 (1965).

¹⁹ In the case of ρ^- production $T=0$ exchange is possible in addition to one-pion exchange; this is not possible in ρ^0 production. See I. Derado, J. A. Poirier, N. N. Biswas, N. M. Cason, V. P. Kenney, and W. D. Shephard, *Phys. Letters* **24B**, 112 (1967).

C. Effects from a Possible s -Wave Resonance

The strong asymmetries observed in ρ^0 decay at lower energies have previously been discussed in terms of interference between the ρ^0 and a $T=0$ d - or s -wave interaction amplitude.^{20,21} In recent theoretical and experimental work, evidence has been presented for a $T=0$ s -wave resonance at about 720 MeV.^{13,18,22} Since the ρ^0 at 8 GeV shows decay asymmetries very similar to those at lower energies, we discuss our data in terms of such an s -wave interaction.

It is now generally believed that the $T=0$ s -wave $\pi\pi$ phase shift is large in the ρ mass region, but it is less clear whether there is an s -wave resonance. Since both experimentally¹³ and theoretically²² the ratio S/P seems to be only a few percent in this region, it is difficult to establish the nature of the s -wave effects. The small magnitude for the S/P ratio comes primarily from an isospin factor of $4/9$ for s -wave compared to p -wave $\pi^+\pi^-$ production, and an angular-momentum factor of $1/3$. These factors combine to give a theoretical weight of $4/27$ for s -wave relative to p -wave resonances decaying to $\pi^+\pi^-$. In addition, if the width of the s -wave resonance were one-third the width of the ρ , as suggested by the experimental evidence of Ref. 18, the expected S/P ratio would be even smaller (assuming similar Δ^2 dependence and form-factor effects for the two resonances).

We have looked for a shift of the " ρ^0 " peak to lower masses as Δ^2 decreases, as reported at lower energies by Hagopian *et al.*² The $\pi^+\pi^-$ mass distributions for three different Δ^2 ranges are shown in Fig. 2. For the lower Δ^2 region the central mass value is slightly lower, but the shift is not statistically significant.

The experimental points for $\text{Re}(\rho_{00}^{\text{int}})$, Fig. 9, seem to fall more rapidly with increasing Δ^2 than the theoretical curve¹⁶ calculated assuming properties for the s -wave resonance similar to the ρ^0 . This suggests a steeper Δ^2 dependence for the s -wave $\pi\pi$ scattering than for the p wave, and contrasts with the situation²³ at 2.7 GeV where $\text{Re}(\rho_{00}^{\text{int}})$ remains relatively constant with increasing Δ^2 .

IV. f^0 MASS REGION

A. Δ^2 Distribution for the f^0 Production Cross Section

Figure 10 shows the Δ^2 distribution of the f^0 cross section. The mass interval is taken from 1170 to 1370 MeV. The absolute scale has been normalized to our estimate of the f^0 total production cross section given in Table I.

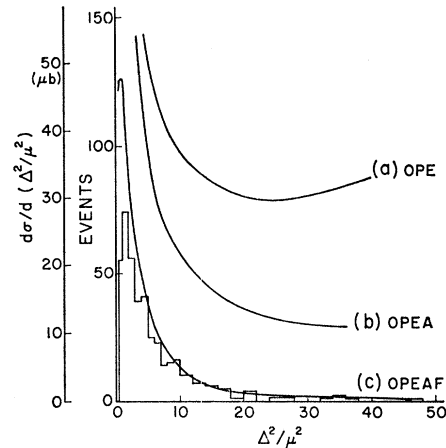


Fig. 10. Production cross section $d\sigma/d(\Delta^2/\mu^2)$ for the f^0 . The solid curves and the predictions of (a) pure one-pion exchange, (b) one-pion exchange with absorption, and (c) one-pion exchange with absorption and form factor.

The theoretical curves in Fig. 10 are (a) pure OPE,²⁴ (b) OPEA,²⁵ and (c) OPEA with a form factor suggested by Yock and Gordon²⁶ (OPEAF). The pure OPE differential cross section is much larger than the observed cross section. Similarly, the OPEA model gives a cross section larger than the observed cross section by more than a factor of two. The shape predicted by the OPEA model is in better agreement with the data than that predicted by the OPE model, but the experimental data have a steeper Δ^2 dependence than predicted by either the OPE or OPEA models. Better agreement is provided by the calculation which includes both absorption and form-factor effects, although the agreement is unsatisfactory for $\Delta^2 < 2 \mu^2$. This is in contrast to the case of the ρ^0 , where both the magnitude and the Δ^2 dependence of the production cross section are well fitted by OPEA without introducing form factors.

It should be noted that other factors can appreciably affect agreement between experiment and theory for f^0 production. There is a substantial background in the f^0 mass region (about 34%). If the background adjacent to the f^0 region is primarily d wave, then our estimate of the fraction of background in the f^0 region is too high and our estimate of the experimental cross section will increase, bringing it closer to the OPE and OPEA curves.

A second factor which would reduce the discrepancy between the data and the OPEA model would be inelastic $\pi\pi$ scattering in the f^0 mass region. In this case, the curves of Fig. 10 would have to be multiplied by a factor less than unity to account for the inelasticity.

²⁰ V. Hagopian and W. Selove, Phys. Rev. Letters **10**, 533 (1963).

²¹ Saclay-Osney-Bari-Bologna Collaboration, Nuovo Cimento **29**, 515 (1963).

²² L. Durand and Y. T. Chiu, Phys. Rev. Letters **14**, 329 (1965).

²³ D. H. Miller, L. Gutay, P. B. Johnson, F. J. Loeffler, R. L. McIlwain, R. J. Sprafka, and R. B. Willman, Phys. Rev. **153**, 1423 (1967).

²⁴ H. Hogaasen, J. Hogaasen, R. Keyser, and B. E. J. Svensson, Nuovo Cimento **42**, 323 (1966).

²⁵ H. Hogaasen (private communication). In this calculation, the absorption parameters A and C [see Ref. 24, Eqs. (3.4) and (3.5b)] are $A_i=7.6$, $A_f=9.0$, $C_i=0.75$, and $C_f=1.0$. The coupling constant $(g_{f\pi\pi})^2/4\pi=3.8$, which corresponds to the full f^0 width $\Gamma_{f^0}=163$ MeV.

²⁶ P. C. M. Yock and D. Gordon, Phys. Rev. **157**, 1362 (1967).

TABLE III. Density matrix elements for the f^0 at 8 GeV/c.

	$\Delta^2 \leq 5 \mu^2$			$5 \mu^2 < \Delta^2 \leq 15 \mu^2$			$\Delta^2 \leq 15 \mu^2$		
	Exp.	OPEA	OPEAF	Exp.	OPEA	OPEAF	Exp.	OPEA	OPEAF
ρ_{00}	0.98 ± 0.09	0.87	0.88	0.82 ± 0.11	0.84	0.81	0.93 ± 0.07	0.85	0.83
ρ_{11}	0.26 ± 0.03	0.06	0.06	0.26 ± 0.04	0.07	0.08	0.26 ± 0.02	0.07	0.08
ρ_{22}	-0.25 ± 0.03	0.00	...	-0.16 ± 0.04	0.00	...	-0.22 ± 0.02	0.00	...
$\rho_{2,-2}$	0.04 ± 0.04	0.00	0.00	-0.02 ± 0.05	0.00	0.01	0.05 ± 0.04	0.00	0.00
$\rho_{1,-1} + (\frac{1}{3}\sqrt{6}) \text{Re}(\rho_{20})$	0.12 ± 0.09	0.01	0.01	0.05 ± 0.05	0.02	0.01	0.12 ± 0.04	0.01	0.01

However, available evidence does not indicate any appreciable inelasticity.²⁷

Finally, it should be noted that the theoretical cross sections depend linearly on the f^0 width, Γ . We have used $\Gamma = 163$ MeV in the calculations. If we use the compilation value of 117 MeV²⁸ for the width, then the theoretical cross sections will be reduced by a factor of 0.72.

B. Decay Angular Distribution

Figure 11 shows the scatter plot of $\cos\theta$ versus α with projections along the axes. The f^0 mass interval is taken from 1170 to 1370 MeV. In contrast to the ρ^0 case, the f^0 angular distributions are more symmetric in $\cos\theta$ and α . The asymmetry parameter in $\cos\theta$, $(F-B)/(F+B)$, is 0.14 ± 0.04 . (For $\Delta^2 \leq 15 \mu^2$, the ratio is 0.10 ± 0.05 .)

Distortion of the f^0 angular distribution due to formation of the $N^{*+}(1236)$ isobar has been discussed by Lee *et al.*⁵ The N^{*+} production in our data is small, and we estimate that it can only account for about one-third of the asymmetry. The effect is probably due primarily to $\pi\pi$ diffraction scattering which can be seen to produce a $\cos\theta$ asymmetry in Fig. 5 which increases as $M(\pi\pi)$ increases. This asymmetry has been discussed in detail elsewhere.²⁹

In order to compare the data with the predictions of the OPEA model and the OPEAF model for the f^0 decay angular distribution, we fitted our data by a least-squares fit to the decay angular projections to obtain some of the density matrix elements ρ_{mn} . The angular distribution for the f^0 ($J^{PC} = 2^{++}$) has the form²⁴

$$\begin{aligned}
 W(\theta, \alpha) = & (15/16\pi) [\sin^4\theta (\rho_{22} + \rho_{2,-2} \cos 4\alpha) \\
 & + \sin^2 2\theta (\rho_{11} - \rho_{1,-1} \cos 2\alpha) + 3\rho_{00} (\cos^2\theta - \frac{1}{3})^2 \\
 & - 4 \sin^2\theta \cos\theta (\text{Re}\rho_{21} \cos\alpha - \text{Re}\rho_{2,-1} \cos 3\alpha) \\
 & + (2\sqrt{6}) \text{Re}\rho_{20} \sin^2\theta (\cos^2\theta - \frac{1}{3}) \cos 2\alpha \\
 & - (2\sqrt{6}) \text{Re}\rho_{10} \sin 2\theta (\cos^2\theta - \frac{1}{3}) \cos \alpha]. \quad (5)
 \end{aligned}$$

Here ρ_{00} , ρ_{11} , and ρ_{22} were obtained from our data for the interval $\Delta^2 \leq 15 \mu^2$, by fitting Eq. (5) integrated over α ;

$\rho_{2,-2}$ and $\rho_{1,-1} + (\frac{1}{3}\sqrt{6}) \text{Re}\rho_{20}$ were similarly obtained by integrating Eq. (5) over $\cos\theta$. In these calculations we have used the normalization condition $\rho_{00} + 2\rho_{11} + 2\rho_{22} = 1$. The results are presented in Table III together with the theoretical predictions of the OPEA²⁴ and the OPEAF²⁶ models.

The values obtained for ρ_{00} and $\rho_{2,-2}$ are in good agreement with the theoretical values. The values of ρ_{11} and $\rho_{1,-1} + (\frac{1}{3}\sqrt{6}) \text{Re}\rho_{20}$, however, are not in good agreement with either theory. Furthermore, our data show a negative value of ρ_{22} , which, for a pure spin 2 state, must be positive. (A negative value of ρ_{22} was also obtained by Cohn *et al.*³⁰) This result indicates that there is appreciable non- d -wave background present in the f^0 region which may be responsible for the discrepancies between theory and the experimental values for ρ_{11} and $\rho_{1,-1} + (\frac{1}{3}\sqrt{6}) \text{Re}\rho_{20}$.

V. g^0 MESON

Data on the g meson at ~ 1650 MeV have been summarized at the International Conference at Berkeley from a collection of many sets of relevant data.³ The isospin of the g is $T \geq 1$ and its spin is not known. Recent experimental data³¹ show that there are three

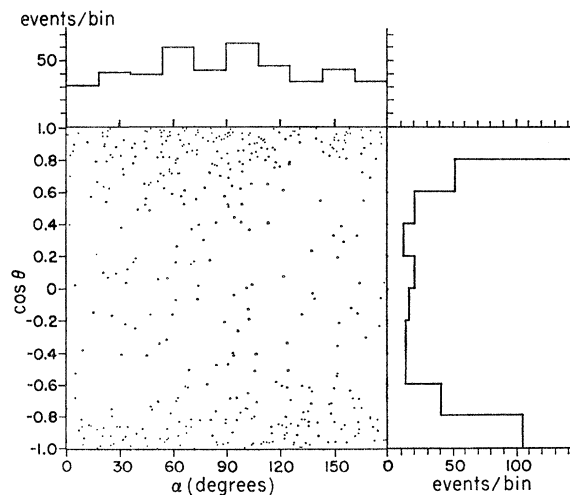


FIG. 11. Scatter plot of $\cos\theta$ versus α for the f^0 with histogram projections on the $\cos\theta$ and α axes.

²⁷ V. Hagopian, thesis, University of Pennsylvania, 1963 (unpublished).

²⁸ A. H. Rosenfeld, A. Barbaro-Galtieri, W. J. Podolsky, L. R. Price, P. Soding, C. G. Wohl, M. Roos, and W. J. Willis, *Rev. Mod. Phys.* **39**, 1 (1967).

²⁹ N. N. Biswas, N. M. Cason, I. Derado, V. P. Kenney, J. A. Poirier, and W. D. Shephard, *Phys. Rev. Letters* **18**, 273 (1967).

³⁰ H. O. Cohn, R. D. McCulloch, W. M. Bugg, and G. T. Condo, *Nucl. Phys.* **82**, 690 (1966).

³¹ M. N. Focacci, W. Kienzle, B. Levrat, B. C. Maglic, and M. Martin, *Phys. Rev. Letters* **17**, 890 (1966).

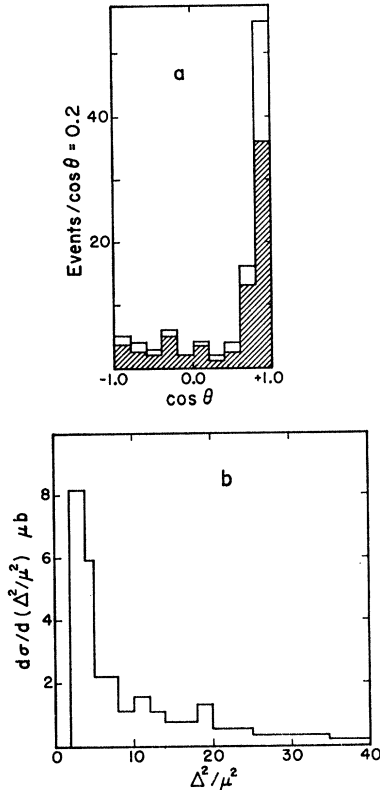


FIG. 12. Decay angular distribution for the g^0 meson. The upper histogram is a histogram of $\cos\theta$ for events with $M(\pi\pi)$ in the interval 1550 to 1750 MeV. The lower shaded histogram is the result of subtracting a normalized background; see text.

resonances around the g -meson mass region; other data³² show a 4π resonance at the g -mass region.

Because of the bias in the Pennsylvania data for this mass region (see Sec. I), we do not present an analysis of the g^0 from the combined data. The following discussion was prepared by the Notre Dame group from an analysis of their data. It is difficult to draw detailed conclusions due to the limited statistics and background uncertainties.

In an attempt to determine the spin of the g^0 meson, we have analyzed the $\cos\theta$ distribution in the g^0 region. Figure 12(a) shows, in the upper histogram, the $\cos\theta$ distribution for the 101 events in the Notre Dame sample with $M_{\pi\pi}$ in the interval 1600–1750 MeV. We have estimated the background in the g^0 region by assuming that it is similar to the combined distribution for events in the adjoining mass regions $1500 \leq M_{\pi\pi} \leq 1600$ MeV and $1800 \leq M_{\pi\pi} \leq 1900$ MeV. This distribution was then normalized to our estimate of the

total background in the 1600–1750-MeV interval (see the cross-section values of Table I). The shaded histogram is then an estimate of the g^0 -meson decay angular distribution after the background subtraction.

The distribution is consistent with isotropy for $\cos\theta < +0.6$, and has a pronounced forward peak. Whether this peak represents a real asymmetry for the g^0 decay due to interference effects, or is due to a large underestimate³³ of a background which is very forward scattered for high $M_{\pi\pi}$, is difficult to determine with the present statistics. In any case, we can draw no conclusions about the spin of the g^0 from this analysis. Figure 12(b) shows $d\sigma/d\Delta^2$ for the same events, $1600 \leq M_{\pi\pi} \leq 1750$ MeV, normalized to the g^0 cross section of Table I.

VI. CONCLUSIONS

We have studied the reaction $\pi^-p \rightarrow \pi^- \pi^+ n$ at 8 GeV/c, and have observed the production of ρ^0 , f^0 , and g^0 mesons. The data in the ρ^0 and f^0 regions have been analyzed primarily in terms of the one-pion-exchange model with absorption (OPEA).

The predictions of the OPEA model are in good agreement with the observed differential production cross section for the ρ^0 . The ρ^0 decay angular distributions exhibit asymmetries comparable to those observed at lower energies. Density matrix elements for the ρ^0 region have been determined assuming that the asymmetries are due to a $T=0$ s -wave $\pi\pi$ interaction. The density matrix elements which do not involve s - p interference are in reasonable agreement with predictions based on the OPEA model. The s - p interference term $\text{Re}(\rho_{00}^{\text{int}})$ is definitely nonzero at low Δ^2 and appears to decrease rapidly with increasing Δ^2 . The data are not inconsistent with the existence of an s -wave resonance; however, no statistically significant conclusions about the existence or properties of such a resonance can be drawn.

For the f^0 meson the experimental production differential cross section is significantly lower, and falls more steeply with increasing Δ^2 , than the predictions of OPEA and simple OPE models. The data are in reasonably good agreement with a recent calculation using OPEA along with form-factor effects. We have obtained values for some of the density matrix elements assuming a pure 2^+ decay of the f^0 . Our data give a negative value for ρ_{22} which theoretically should be positive. Disagreement between experimental and theoretical values for the matrix elements indicates the importance of effects from the substantial nonresonant background present in this mass region.

³² W. J. Kernan, D. E. Lyon, and H. B. Crawley, Phys. Rev. Letters **15**, 803 (1965); F. Conte, G. Tomasini, P. Dittman, G. Drews, P. VanHandel, H. Nagel, L. Mandelli, S. Ratti, A. Silvestri, G. Vegni, P. Daronian, A. Dandin, C. Cochowski, and C. Lewin, Phys. Letters **22**, 702 (1966); T. H. Groves, J. W. Andrews, N. N. Biswas, N. M. Cason, I. Derado, V. P. Kenney, J. A. Poirier, and W. D. Shephard, Bull. Am. Phys. Soc. **12**, 487 (1967).

³³ It should be noted that the fit used to determine the g^0 production cross section was strongly influenced by a dip in the $\pi\pi$ mass distribution near 1500 MeV which might be a statistical fluctuation or might indicate f^0 - g^0 interference. As a consequence, the background in the g^0 -mass region may be underestimated. A large increase in the background would, however, be required, to eliminate the observed forward peak in $\cos\theta$.

The g^0 meson observed in our data at 1680 MeV is consistent with the previously reported resonances. Our data are too limited in statistical accuracy to determine uniquely the spin of the g^0 .

ACKNOWLEDGMENTS

This experiment was made possible by the help and cooperation of the Shutt bubble chamber group and the AGS personnel of Brookhaven National Laboratory. Particular thanks are due to Dr. D. Rahm and Dr. M. Webster for their assistance with the beam. We are grateful to Dr. R. Jabbur of Argonne National Laboratory for providing helpful calculations. We wish to

acknowledge the assistance of J. B. Annable, R. J. Schlentz, and the Notre Dame scanning and measuring staff, R. Marshall, R. VanBerg, W. Kononenko, F. Forman, and the Pennsylvania scanning and measuring staff, with the data analysis. The cooperation of the Notre Dame, Pennsylvania, and New York University Computer Centers is appreciated. J. W. Andrews and J. W. Lamsa assisted in the preparation of these data. The Pennsylvania group wishes to thank Dr. V. Hagopian, Dr. H. Brody, and Dr. Y. L. Pan for their advice and help throughout this experiment. One of us (H. Y.) would like to thank the Rochester bubble chamber group, especially Dr. T. Ferbel, for helpful discussions.

PHYSICAL REVIEW

VOLUME 163, NUMBER 5

25 NOVEMBER 1967

Nucleon-Nucleon Polarization between 300 and 700 MeV*

DAVID CHENG AND BURNS MACDONALD†

Lawrence Radiation Laboratory, University of California, Berkeley, California

AND

JEROME A. HELLAND

University of California, Los Angeles, California

AND

PHILIP M. OGDEN

Seattle Pacific College, Seattle, Washington

(Received 23 January 1967)

The polarization parameter $P(\theta^*)$ has been measured at beam energies of 310, 400, 500, 600, and 700 MeV over the range in the c.m. scattering angles $30 \text{ deg} \leq \theta^* \leq 150 \text{ deg}$ to an accuracy of typically ± 0.03 for pn scattering, and ± 0.02 for pp scattering. A polarized proton beam was scattered from an unpolarized target—deuterium for quasifree pn and pp measurements, hydrogen for free pp measurements—and both of the outgoing nucleons from the (quasi-) elastic scatter were detected by an array of 27 scintillation counters in multichannel coincidences. It was found that $P(\theta^*)$ for pp scattering can be approximated by $A \sin\theta^* \cos\theta^*$, where A varies from -0.25 at 310 MeV to -0.4 at 700 MeV in this range. A comparison of $P(\theta^*)$ for free and quasifree pp scattering reveals good agreement between the two.

I. INTRODUCTION

NUCLEON-NUCLEON (NN) scattering amplitudes are determined experimentally by scattering experiments involving cross sections and/or polarizations. At low energies, where inelastic processes are not important, these amplitudes are conveniently parametrized at each energy and all angles by a set of real phase shifts and mixing parameters. However, at higher energies, not only do more phase shifts of higher angular momentum states contribute to the scattering, but also the phase shifts become complex because of the opening of inelastic channels. Therefore, phase-shift analysis becomes extremely difficult and impractical, and its physical significance becomes less

apparent. An alternative scheme as a meeting ground between experimental data and theoretical models has been proposed by Wolfenstein.¹ In the pp system, there are five complex (Wolfenstein¹) amplitudes which are functions of energy and c.m. angle, θ^* , ($0 \leq \theta^* \leq \pi/2$). (See Appendix.) These amplitudes have symmetry properties about $\theta^* = \pi/2$. In order that these five complex amplitudes be determined experimentally at a given energy and angle, at least nine linearly independent observables (such as differential cross section, polarization, and rotation parameters) must be measured to solve for nine of the ten real quantities in the five complex amplitudes. (One phase is arbitrary.²)

¹ L. Wolfenstein and J. Ashkin, *Phys. Rev.* **85**, 947 (1952).

² The over-all phase is not determined from this formalism because the amplitudes are bilinear in the observables. However, the phase can be determined from the optical theorem relating the imaginary part of the scattering amplitude to the total cross section.

* Work supported by the U. S. Atomic Energy Commission.

† Present address: Virginia Polytechnic Institute, Blacksburg, Virginia.